ISSN: 0369-8963

C_3N_4 HYBRIDISED $ZNBI_2O_4$ (G-C_3N_4/$ZNBI_2O_4$) NANORODS FOR ANTIBACTERIAL ACTIVITY AND CYTOTOXICTY ANALYSIS

AYYAPPAN S[1*] & NITHYA R[2]

[1*]Associate Professor, Government College of Engineering, Salem, Tamil Nadu, India
[2] Research Scholar, Government College of Engineering, Salem, Tamil Nadu, India

ABSTRACT

The synthesis of g-C_3N_4 nanorods via chemical exfoliation involves breaking down bulk g-C_3N_4 into nanorods, enhancing their surface area and reactivity. The coupled g-C_3N_4/$ZnBi_2O_4$ nanocomposite, prepared through a cost-effective hydrothermal method, likely facilitates synergistic effects that improve antibacterial and cytotoxic activities. For evaluating antibacterial efficacy, you can culture Escherichia coli and Staphylococcus aureus to test the response of both the pure g-C_3N_4 nanorods and the g-C_3N_4/$ZnBi_2O_4$ nanoparticles.

Keywords: ***Graphitic Carbon Nitride, zinc bismuthate, Staphylococcus aureus, Escherichia coli and Cytotoxicity***

1. INTRODUCTION

The discovery of g-C_3N_4 as a metal-free conjugated semiconductor photocatalyst for H_2 evolution [1]. This potentially shifted the research exploration from inorganic to polymeric conjugated semiconductor photocatalysts. There are generally seven phases of C_3N_4, which are α-C_3N_4, β-C_3N_4, cubic C_3N_4, pseudo cubic C_3N_4, g-h-triazine, g-o-triazine, and g-h-heptazine with band gaps of around 5.49, 4.85, 4.30, 4.13, 2.97, 0.93, and 2.88 eV, respectively. It was found that the basic tectonic units to establish allotropes of g-C_3N_4 are triazine (C_3N_3) and tri-s-triazine/heptazine (C_6N_7) rings. In this case, the size of the nitride pores and the different electronic environments of the N atom contribute to various energetic stabilities. Among all phases, tri-s-triazine based g-C_3N_4 was energetically favored and was the most stable phase of C_3N_4 at ambient conditions. This was in line with the first-principles density functional theory (DFT) calculations performed [2]. Most works indicated that the poly condensation of melamine, cyanamide, dicyandiamide, or urea formed a melon polymer from the melem units, manifesting that the tectonics was the most stable pattern. Thus, the tri-s-triazine is generally recognized as the building block for the typical formation of g-C_3N_4.

Polymeric g-C_3N_4 consists of earth-abundant carbon and nitrogen elements; it is versatile for providing reactions to alter its surface activity without manifestly changing the

 https://doi.org/10.5281/zenodo.14065498

ISSN: 0369-8963

theoretical structure and composition. Due to the polymeric feature of g-C_3N_4, the surface chemistry can be easily modulated by means of surface engineering at the molecular level. Furthermore, it has the lowest band gap among the seven phases of C_3N_4, owing to the presence of sp^2-hybridized carbon and nitrogen, establishing the π-conjugated electronic structures. In comparison with TiO_2, g-C_3N_4 has a moderate band gap of 2.7−2.8 eV, resulting in an onset visible light absorption of around 450−460 nm. As the most stable allotrope in all C_3N_4 structures, g-C_3N_4 is thermally stable up to 600°C in air, as evidenced by thermo gravimetric analysis (TGA), which can be ascribed to the aromatic C−N heterocycles. In addition to that, g-C_3N_4 is also chemically stable and not dissolved in acid, alkali, or organic solvents, rendering it a robust material under ambient conditions.

Highly toxic aromatic organic compound like Phenol and its derivatives are widely disseminated and likely to be present highly in the natural environment. In particular, 4-Nitrophenol is nitroaromatic compounds possess carcinogenic nature causes considerable damage to the eco-system and human and is considered to be priority, bio-refractory pollutant by USEPA in many countries [3]. 4-Nitrophenol is mainly used in the manufacture of various fungicides, therapeutic drugs, the dyes to darken leather and it is produced in large quantities worldwide. The maximum allowed concentration of 4-Nitrophenol in water is in the range of 1-20 ppb [4]. Various biohazards like bacteria and viruses are widely existent in the water sources and pose significant vulnerabilities to human and healthy eco-system. Water disinfection is mainly attained through chlorination or ozonation in water plants, but, the formation of potentially carcinogenic disinfection by-products is the main concern [5]. Increased usage of high dosages of chemical decontaminators for inactivation of bacteria and viruses lead to the formation of more disinfection by-products [6]. Photocatalytic degradation is the promising method for the purification and treatment of industrial wastewater. The development of cost-effective, non-toxic and earth-abundant and visible-light-driven recyclable photocatalysts is still a major challenge. Nowadays, exploration of suitable semiconductor photocatalysts for effective utilization of solar energy towards chemical energy is one of the noble tasks to the scientific community [7]. Semiconductor nanoparticles with a suitable bandgap and flat band potential are commonly used as photocatalysts. In recent years, polymeric metal-free graphitic carbon nitride (g-C_3N_4) has become a new class of organic semiconductor that has significant applications in (photo) catalysis, energy and environmental remediation [8].

The pristine metal-free 1D g-C_3N_4 exhibit excellent photo stability and narrow band emission that helps to tailor their functionalities also has several shortcomings like low visible light absorption rapid recombination rate [9]. Researchers worldwide are made efforts to address these shortcomings by various strategies. Recently, Dana et.al reported the H_2O_2 functionalised g-C_3N_4-based nano photocatalyst with enhanced activity [10]. Wu et.al has developed soluble g-C_3N_4

 https://doi.org/10.5281/zenodo.14065498

ISSN: 0369-8963

nanosheets with excellent dispensability for improved H_2 production [11]. Stacking of co-catalysts onto the surface of a catalyst could evidently improve the separation efficiency and thereby enhances the photocatalytic behaviour in the heterogeneous photocatalytic system (Tahir and others). Easy and fast separation of the photocatalyst from the contaminated solution after photoreaction is critical in photocatalytic applications [12]. Hierarchically porous magnetically separable g-C_3N_4/Fe_3O_4/$CoMoO_4$ photocatalyst with enhanced textural properties were reported [13].

Recently, $ZnBi_2O_4$ (zinc bismuthate) have attracted attention among many researchers due to its potential applications in diverse fields such as optoelectronics and photocatalysis. It is a direct bandgap semiconductor with bandgap in the range of 3.1 – 3.6eV. The crystalline structure of $ZnBi_2O_4$ possesses zigzag metal-oxygen chains made up of edge-sharing Zn and Bi atoms [14]. Recently, Huy et.al reported the graphite modified $ZnBi_2O_4$ nanostructures [15]. Very few reports were available on the exploitation of g-C_3N_4/$ZnBi_2O_4$ for various applications. Hence, our proposed work demonstrates the synthesis of 1D graphitic carbon nitride nanostructures by liquid-phase exfoliation and g-C_3N_4 embedded $ZnBi_2O_4$ nanorods by the cost-effective hydrothermal method using CTAB as the capping agent for the first time (soft template synthesis). The photocatalytic and antimicrobial properties of the obtained g-C_3N_4 and g-C_3N_4/ $ZnBi_2O_4$ nanoparticles were analyzed.

Graphitic Carbon Nitride (G-C_3N_4)

Transition metal carbides and nitrides of groups (IV-VI) have been attracting much attention because of their distinctive chemical and physical properties. Graphitic Carbon Nitride (g-C_3N_4) has attracted significant interest in the last few years as a low-cost alternative to metal-based materials in many fields due to its low cost, environmentally benign nature, easy synthesis and tunable properties.

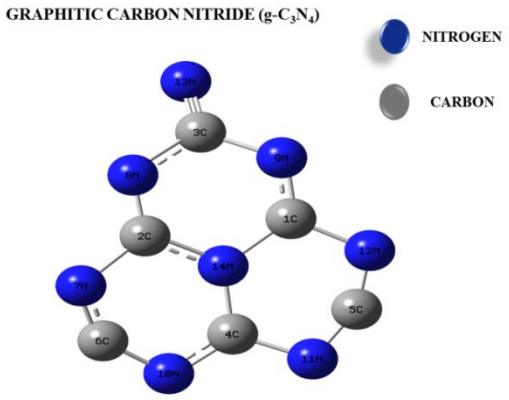

Fig 1 Model of Graphitic Carbon Nitride (G-C_3n_4)

https://doi.org/10.5281/zenodo.14065498

ISSN: 0369-8963

The g-C_3N_4 is regarded as considered as the stable allotrope of carbon nitride family under ambient conditions. It has a stacked 2d structure with each layer composed of conjugated planes connected through sp^2 hybridization of carbon and nitrogen atoms. The g-C_3N_4 is a yellow-colored semiconductor, with a bandgap around 2.7eV.

Several complications relates to infectious diseases have significantly decreased due to the availability and use of a wide variety of antibiotics and antimicrobial products. An excessive use of antibiotics and antimicrobial agents over years has increased the number of drug resistant pathogens. Microbial multidrug resistance possess risks and research attention has focused on finding alternatives for antimicrobial treatment. Among the various approaches, the use of nanostructures is the most promising strategy to overcome microbial drug resistance due to their high surface-to-volume ratio and chemically incorporated antibacterial activity. Graphene, a two-dimensional nanomaterial, possesses excellent biocompatibility, putting it in the forefront for different applications in bio sensing, drug delivery, biomedical device development, diagnostics and therapeutics [16]. Graphene-based nanostructures also hold great promise against microbial infections. Anti-bacterial activities of the samples were performed against both Gram-negative (*E. coli*) and Gram-positive (*S. aureus)* and moderate zone of inhibition was observed for all the samples. Anti-fungal activities of the samples were performed against candida albicans [17,18]. The antimicrobial activity of all the series powder sample is done by modified Kirby-Bauer disk diffusion method. Anti-Bacterial efficiency against both Gram-positive (*S. aureus*) and Gram-negative (E. coli) bacterial and anti-fungal candida albicans were studied, The present research focuses on ways to achieve simple and cost-effective green synthesis of exfoliated g-C_3N_4 it with novel binary metal oxides ($ZnBi_2O_4$) to enhance Antimicrobial and in vitro cytotoxic activity.

Gram-negative and Gram-positive bacteria

Bacteria are microscopic single-celled organisms that thrive in diverse environments. They can live within soil, in the ocean and inside the human gut. Human’s relationship with bacteria is complex. Sometimes they lend a helping hand, by curdling milk into yogurt or helping with our digestion. At other times they are destructive, causing diseases like pneumonia. In the present work the antibacterial activity of as synthesized nanoparticles against two Gram positive (Staphylococcus aureus) and Gram negative (Escherichia coli) bacterial strains were studied.

Staphylococcus aureus (S.aures) is a gram-positive bacterium found in the nose, respiratory tract and on the skin. It can cause a range of illnesses, from minor skin infections to life threatening diseases such as pneumonia, meningitis, osteomyelitis, endocarditis, toxic shock syndrome, bacteraemia and sepsis.

 https://doi.org/10.5281/zenodo.14065498

ISSN: 0369-8963

Escherichia coli, also known as E.coli is a gram negative, anaerobic, rod shaped bacterium of the genus Escherichia is commonly found in the lower of warm blooded organisms which causes the majority of urinary tract infections.

2. MATERIALS AND REAGENTS

Thiourea, Zinc nitrate [Zn $(NO_3)_2.6H_2O$], Bismuth nitrate [Bi $(NO_3)_3.5H_2O$], CTAB, NaOH, H_2SO_4 and Ethanol was purchased from Merck. All chemical purchased were of analytical grade and used without further purification.

Synthesis of Bulk Graphitic carbon nitride (g-C_3N_4)

The polymeric metal-free Graphitic carbon nitride (g-C_3N_4) nanoparticles were prepared by poly-condensation of thiourea at 500 ˚C for 3 hrs in an air atmosphere. Thiourea is readily available in the industry at low cost. In a typical process, a 10g of thiourea was put into a closed alumina crucible with a cover and then heated to 500 ˚C in a muffle furnace for 3 hrs at a heating rate of 10 ˚C min^{-1}. After the reaction, the alumina crucible was cooled to room temperature. The resultant g-C_3N_4 solid product was collected and ground into a fine powder respectively. Obtained yellow-colored fine particles were washed using distilled water to remove the alkaline residue and dried at 60 ˚C.

1D g-C_3N_4 nanorods were prepared by chemical exfoliation of bulk g-C_3N_4. In the present work, bulk g-C_3N_4 was exfoliated by means of adding 0.1M of H_2SO_4 into distilled water suspension. Nearly 5g of bulk g-C_3N_4 was added to the 100ml deionized water and stirred using magnetic stirrer for about 45 minutes to obtain a homogenous mixture and H_2SO_4 was added dropwise. Then, this mix was kept under ultrasonication by using probe sonicator for about 5 hrs. After the time, mix was taken out and centrifuged. Precipitate was collected and washed several times with ethanol and deionized water to remove the residue and dried at 60˚C for 8 hrs. Pale-yellow colored fine crystalline nanoparticles were obtained.

Synthesis of g-C_3N_4-$ZnBi_2O_4$ nanocomposite

In the present work, g-C_3N_4 coupled $ZnBi_2O_4$ nanocomposite was prepared by cost-effective hydrothermal method. In a typical process, an appropriate amount of 0.5M g-C_3N_4 was dissolved in 100ml deionized water sonicated for about 45 min to obtain homogenous dispersion. To the above aqueous dispersion of g-C_3N_4, 50ml of analytical grade 0.7M Zn $(NO_3)_2.6H_2O$ and 0.3M Bi $(NO_3)_3.5H_2O$ were added under magnetic stirring. Under continuous stirring, an appropriate amount of 0.05M CTAB was poured on to the solution mix and pH of the above solution was maintained at pH 10 by the dropwise addition of 0.05M NaOH. After stirring for about 1 hr, homogenous mix was transferred to Teflon lined autoclave and maintained at 150˚C for 14 hrs. After the process, the autoclave was allowed to cool at room temperature. Yellowish white powder was obtained and

 https://doi.org/10.5281/zenodo.14065498

ISSN: 0369-8963

washed several times with deionized water and ethanol in order to remove the alkaline substances on the surface of the nanoparticles and dried in an air atmosphere. This experimental process was adopted to prepare the three different molar concentrations (3, 5 and 7 mol %) of $ZnBi_2O_4$ on g-C_3N_4.

Nucleation and growth mechanism

In this study, we present the simple hydrothermal synthesis of g-C_3N_4/$ZnBi_2O_4$ nanorods using CTAB as the capping agent. CTAB is a cationic surfactant used as a soft template for the formation of highly oriented nanoparticles [19]. After the dissolution of an appropriate amount of precursors in deionized water, 0.05M % of CTAB was added as the surfactant. When CTAB dissolved in water it gets ionised and form the hexagon-shaped micelle [20]. During the nucleation process, NaOH splits into OH^- and Na^+ ions. Since CTAB is positively charged with tetrahedral head controls the rate of hydrolysis and influences the slow release of OH^- ions [21]. Anionic ions of Bi^+ get attached to cations of CTAB. When the pH of the solution mix reaches to 10, the solubility product attains supersaturation and favours the homogenous nucleation of g-C_3N_4 on to porous $ZnBi_2O_4$ and oxidation of hydroxyls. CTAB prevents further aggregation and due to high surface energy of 1D g-C_3N_4 nanoparticles and temperature, the hexagon-shaped micelles were elongated to form porous hexagonal rod-like nanostructure with irregular size and high crystallinity.

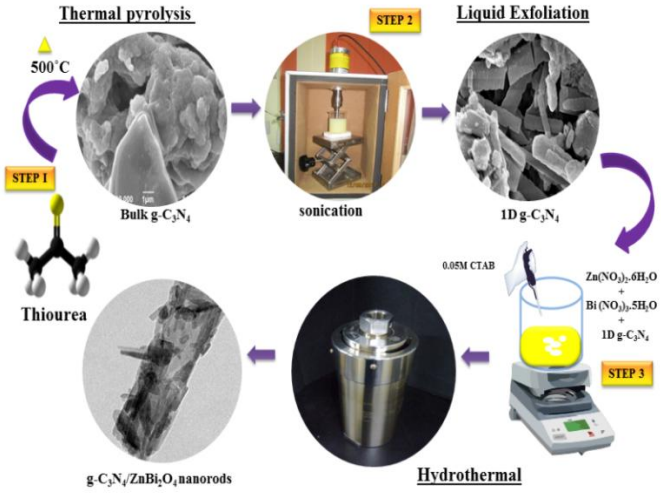

Figure Error! No text of specified style in document**..1 Schematic illustration of preparation of g-C_3N_4/ $ZnBi_2O_4$ nanorods**

3. ANTI-BACTERIAL ACTIVITY

It is demonstrated that carbon-based materials and metal oxide nanoparticles exhibit efficient antimicrobial properties against common water pathogens [22]. In this present work, as-synthesized pristine g-C_3N_4 and g-C_3N_4/$ZnBi_2O_4$ nanocomposite were analyzed its antibacterial properties against Gram-positive and Gram-negative clinical pathogens like E.coli and S.aures bacterial strain.

https://doi.org/10.5281/zenodo.14065498

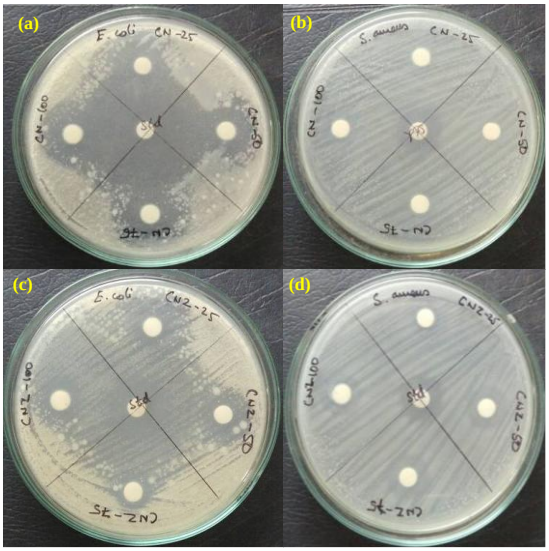

Figure Error! No text of specified style in document.**.13 Antibacterial activities of pure g-C_3N_4 and g-C_3N_4/$ZnBi_2O_4$ nanorods**

Herein our results revealed that $ZnBi_2O_4$ doped g-C_3N_4 showed strong inhibitory activity with higher zone diameter than pristine g-C_3N_4. The g-C_3N_4/$ZnBi_2O_4$ nanocomposite showed a strong Zone of Inhibition (ZOI) against E.coli for 100µg/disk optimal concentration; strong inhibition was due to physicochemical binding of the g-C_3N_4/$ZnBi_2O_4$ nanocomposite on the surface of the bacteria. Antimicrobial properties of the semiconducting heterostructure nano photocatalyst mainly depend on the increased number of highly active chemically reactive oxidant species (ROS) on the heterojunction interface [23]. The fine crystalline structure and incorporation of dopant of the g-C_3N_4/$ZnBi_2O_4$ nanocomposite enhances the photogenerated electron-hole transfer between core shells to the catalyst surface, which enhances the antimicrobial behaviour of as-prepared nanocomposite.

The photogenerated free radicals react with alkaline substances present in the surface and gets converted into hydroxyl ion (OH^-) and super oxide radicals (O_2*) which affects the bacterial cell membrane. It is also observed that the g-C_3N_4 could penetrate the bacterial cells and then inhibit their growth (Bing et.al, 2015). The as-prepared g-C_3N_4/$ZnBi_2O_4$ nanoparticles mainly acts on the outer surface (cell wall) of the bacterial strain and cell wall of a bacteria is a complex structure made of lipopolysaccharide (G -ve) and peptidoglycan (G +ve) [24]. E.coli associated with more anionic groups which electrostatically interact with the polycationic structure of g-C_3N_4/$ZnBi_2O_4$. The g-C_3N_4/$ZnBi_2O_4$ acts as the chelating agent that selectively binds the cations on the cell wall and disrupts the integrity of the membrane [25] Therefore, compare to pristine g-C_3N_4, g-C_3N_4/$ZnBi_2O_4$ nanocomposite substantially decreases bacterial growth towards E.coli than S.aures and a high zone of inhibition was observed for the tested bacteria.

 https://doi.org/10.5281/zenodo.14065498

Table Error! No text of specified style in document.**.1 Antibacterial activity against Gram positive and Gram negative bacterial strain of pure g-C_3N_4 and g-C_3N_4/$ZnBi_2O_4$ nanoparticles**

S.No	Bacterial Strain	Zone of Inhibition(mm)				
		Standard ciprofloxacin (10µg/disc)	Pure g-C_3N_4 nanorods (25 -100µg/disc)			
			25	50	75	100
1.	*Escherichia coli*	56	21	28	31	39
2.	*Staphylococcus aureus*	32	11	14	18	18
g-C_3N_4/$ZnBi_2O_4$ nanoparticles (25 -100µg/disc)						
1.	*Escherichia coli*	61	33	35	41	48
2.	*Staphylococcus aureus*	40	20	19	21	22

4. CYTOTOXICTY ANALYSIS

The dose dependent cytotoxicity test of the rod like g-C_3N_4/$ZnBi_2O_4$ nanoparticles was evaluated against L929 cell line. The percentage of cell viability obtained with continuous incubation for 48 hours for various concentrations is depicted in Fig. L929 cell line was procured from NCCS, Pune, India. Cultured cancer cells are valuable reagents for rapid screening of potential anticancer agents as well as for the elucidation of mechanism of their activity.

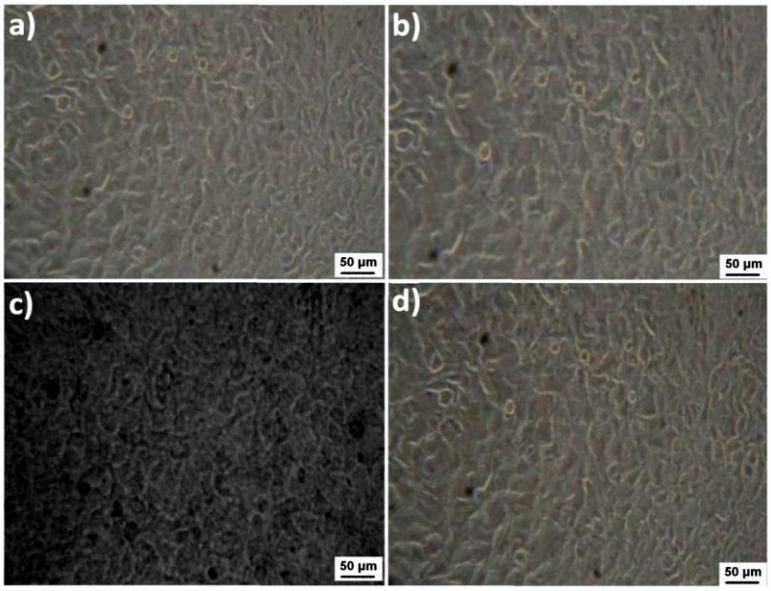

Figure Error! No text of specified style in document.**.14 Cytotoxicity evaluations of g-C_3N_4/$ZnBi_2O_4$ nanorods**

https://doi.org/10.5281/zenodo.14065498

On treatment with compound S51 and control the MOLT-3 cells showed an increased rate of cell death at a volume of 100µl. The compound exhibited 74.1% cell inhibition after 24 h incubation.

CONCLUSION

In summary, we have synthesized exfoliated porous nanorods of metal-free g-C_3N_4 with $ZnBi_2O_4$ metal nanocomposite by the cost-effective hydrothermal method. The higher activity of g-C_3N_4/$ZnBi_2O_4$ nanorods compared to bulk g-C_3N_4 may be due to their enlarged surface area which enhances the photogeneration of active OH^- radicals in water. The results reported in the work may suggest the easy synthesis of fine morphology hybrid, porous metal oxide nanocomposite which can be effectively applied to photocatalytic and antimicrobial applications. The synthesis of $ZnBi_2O_4$-doped g-C_3N_4 nanorods was achieved through a sol-gel assisted precipitation method, utilizing cetyltrimethylammonium bromide (CTAB) as a chelating agent. This method facilitates controlled particle formation and doping, resulting in stable dual-substituted nanoparticles.

The antibacterial activity of these doped g-C_3N_4 and $ZnBi_2O_4$ nanorods was tested against both Gram-positive and Gram-negative bacterial strains, specifically Escherichia coli (E. coli) and Staphylococcus aureus (S. aureus). This testing aimed to evaluate the effectiveness of the nanoparticles in inhibiting bacterial growth in these common pathogens. Additionally, the cell viability and cytotoxicity of g-C_3N_4-substituted $ZnBi_2O_4$ nanorods were estimated using the MTT assay, which provides quantitative data on the metabolic activity of live cells in culture, allowing for the assessment of biocompatibility and potential applications in biomedical fields.

References:

1. Wang, M, Cui, S, Yang, X & Bi, W 2015, ‘Synthesis of g-C_3N_4/Fe_3O_4 nanocomposites and application as a new sorbent for solid phase extraction of polycyclic aromatic 645 hydrocarbons in water samples’, Talanta, vol. 132, pp. 922-928.
2. Liming Sun, Xian Zhao, Chun-Jiang Jia, Yixuan Zhou, Xiufeng Cheng, Pan Li, Li Liu & Weiliu Fan 2012, ‘Enhanced visible-light photocatalytic activity of g-C3N4-ZnWO4 by fabricating a heterojunction: investigation based on experimental and theoretical studies’, J. Mater. Chem. vol. 22, pp. 23428
3. Lin, H, Liu, Y, Deng, J, Xie, S, Zhao, X, Yang, J, Zhang, K, Han, Z, and Dai, H, 2017, ‘Graphitic carbon nitride-supported iron oxides: High-performance photocatalysts for the visible-light-driven degradation of 4-nitrophenol’, Elsevier B, vol.5, pp.105–114
4. Lakshmi, K, Mathusalini, S, Arasakumar, T, Kadirvelu, K, and Mohan, P S, 2017, ‘Highly reactive lanthanum doped zinc oxide nanofiber photocatalyst for effective decontamination of methyl parathion’, Journal of Materials Science: Materials in Electronics, vol. 28, pp. 12944–12955.
5. Kurapati, R, Kostarelos, K, Prato, M, and Bianco, A, 2016, ‘Biomedical Uses for 2D Materials Beyond Graphene: Current Advances and Challenges Ahead’, Advanced Materials, vol.9, pp. 6052–6074.
6. Wang, W, Wong, P, K, Pillai, S, C, Ming, T, and Dunlop, P, S, M, 2016, ‘Photocatalysis in Environment, Energy, and Sustainability’, International Journal of Photoenergy, vol.7, p. 11432.
7. Niu, P, Zhang, L, Liu, G, and Cheng, H, 2012, ‘Graphene-Like Carbon Nitride Nanosheets for Improved Photocatalytic Activities’, Chemistry Select, vol.11, pp. 537 – 541.

 https://doi.org/10.5281/zenodo.14065498

8. Lam, S, Sin, J, and Rahman, A, 2016, 'Materials Science in Semiconductor Processing A review on photocatalytic application of g-C3N4 / semiconductor (CNS) nanocomposites towards the erasure of dyeing wastewater', Materials Science in Semiconductor Processing, vol. 47, pp. 62–84.
9. Ong, WJ, Tan, LL, Ng, YH, Yong, ST & Chai, SP 2016, 'Graphitic carbon nitride (g-C3N4)-based photocatalysts for artificial photosynthesis and environmental remediation: are we a step closer to achieving sustainability? Chem'. Rev. Vol. 116, pp. 7159-7329.
10. Fang, LJ, Li, YH, Liu, PF, Wang, DP, Zeng, HD, Wang, XL & Yang, HG 2017, 'Facile fabrication of large-aspect-ratio g-C3N4 nanosheets for enhanced photocatalytic hydrogen evolution', ACS Sustain. Chem. Eng. vol. 5, pp. 2039-2043.
11. Wu, J, Li, N, Fang, HB, Li, X, Zheng, YZ & Tao, X 2019, 'Nitrogen vacancies modified graphitic carbon nitride: scalable and one-step fabrication with efficient visible lightdriven hydrogen evolution', Chem. Eng. J. vol. 358, pp. 20-29.
12. Liang, Q, Yu, L, Jiang, W, Zhou, S, Zhong, S, and Jiang, W, 2017, 'One-pot synthesis of magnetic graphitic carbon nitride photocatalyst with synergistic catalytic performance under visible-light irradiation', Journal of Photochemistry and Photobiology A: Chemistry, vol. 335, pp. 165–173.
13. Ansari, SA & Cho, MH 2017, 'Simple and large scale construction of MoS_2-g-C_3N_4 heterostructures using mechano chemistry for high performance electrochemical supercapacitor and visible light photocatalytic applications', Sci. Rep. vol. 7, p. 43055.
14. Tho, N, T, M, Phuong, N, T, K, Huy, B, T, Khanh, D, N, N, Ha, H, N, N, Huy, V, Q, Vy, N, T, T, Huy, D, M, and Dat, D, P, 2018, 'Facile synthesis of $ZnBi_2O_4$-graphite composites as highly active visible-light photocatalyst for the mineralization of rhodamine B', Korean Journal of Chemical Engineering, vol. 35, pp. 2442–2451.
15. Huy, B. T, Thao, C, T, B, Dao, V, D, Phuong, N, T, K, and Lee, Y, I, 2017, 'A Mixed-Metal Oxides/Graphitic Carbon Nitride: High Visible Light Photocatalytic Activity for Efficient Mineralization of Rhodamine B', Advanced Materials Interfaces, vol. 4, pp. 1–9.
16. Shandilya, M, Rai, R & Singh, J 2016, 'Review: hydrothermal technology for smart materials', Adv. Appl. Ceram., vol. 115, pp. 354–376.
17. Huang, J, Ho, W, and Wang, X, 2014, 'Metal-free disinfection effects induced by graphitic carbon nitride polymers under visible light illumination', Chemical Communications, vol. 50, pp. 4338–4340.
18. Predoi, D, Iconaru, S, L, Deniaud, A, Chevallet, M, Michaud-Soret, I, Buton, N, and Prodan, A, M, 2017, 'Textural, structural and biological evaluation of hydroxyapatite doped with zinc at low concentrations', Materials, v. 10, pp. 546- 552.
19. Ramadas, M, Bharath, G, Ponpandian, N, and Ballamurugan, A, M, 2017, 'Investigation on biophysical properties of Hydroxyapatite/Graphene oxide (HAp/GO) based binary nanocomposite for biomedical applications', Materials Chemistry and Physics, vol. 199, pp. 179–184.
20. Singh, V, Devi, S, Pandey, V, S, Bharj, R, S, and Tyagi, S, 2018, 'Synthesis and Characterization of Carbon Nanotubes Doped Hydroxyapatite Nanoceramic for Orthopedic Applications', Transactions of the Indian Institute of Metals, vol. 71, pp. 177–183.
21. Maheswari, N, and Muralidharan, G, 2016, 'Hexagonal CeO_2 nanostructures: An efficient electrode material for supercapacitors', Dalton Transactions, vol. 45, pp. 14352–14362.
22. Hamzah, A. A, Selvarajan, R. S, and Majlis, B. Y, 2017, 'Graphene for biomedical applications: A review', Sains Malaysiana, vol. 46, pp. 1125–1139.
23. Han, Z, Wang, N, Fan, H, and Ai, S, 2017, 'Ag nanoparticles loaded on porous graphitic carbon nitride with enhanced photocatalytic activity for degradation of phenol', Solid State Sciences, vol. 65, pp. 110–115.
24. Pant, B, Park, M, Lee, J, H, Kim, H, Y, and Park, S, J, 2017, 'Novel magnetically separable silver-iron oxide nanoparticles decorated graphitic carbon nitride nano-sheets: A multifunctional photocatalyst via one-step hydrothermal process', Journal of Colloid and Interface Science, vol. 496, pp. 343–352.
25. Khadgi, N, Upreti, A, R, and Li, Y, 2017, 'Simultaneous bacterial inactivation and degradation of an emerging pollutant under visible light by $ZnFe_2O_4$ co-modified with Ag and rGO', RSC Advances, vol. 7, pp. 27007–27016.

 https://doi.org/10.5281/zenodo.14065498